Molecular and Cellular Endocrinology 538 (2021) 111471

Contents lists available at ScienceDirect

Molecular and Cellular Endocrinology

journal homepage: www.elsevier.com/locate/mce

Plasmin generates vasoinhibin-like peptides by cleaving prolactin and placental lactogen

Christin Friedrich [a,1], Leon Neugebauer [a,1], Magdalena Zamora [b,a], Juan Pablo Robles [b], Gonzalo Martínez de la Escalera [b], Carmen Clapp [b], Thomas Bertsch [a], Jakob Triebel [a,*]

[a] Institute for Clinical Chemistry, Laboratory Medicine and Transfusion Medicine, Nuremberg General Hospital & Paracelsus Medical University, Nuremberg, Germany
[b] Instituto de Neurobiología, Universidad Nacional Autónoma de México (UNAM), Campus UNAM-Juriquilla, Querétaro, Mexico

ARTICLE INFO

Keywords:
Vasoinhibin
Prolactin
Placental lactogen
Plasmin
16K PRL

ABSTRACT

Vasoinhibin is an antiangiogenic, profibrinolytic peptide generated by the proteolytic cleavage of the pituitary hormone prolactin by cathepsin D, matrix metalloproteinases, and bone morphogenetic protein-1. Vasoinhibin can also be generated when placental lactogen or growth hormone are enzymatically cleaved. Here, it is investigated whether plasmin cleaves human prolactin and placental lactogen to generate vasoinhibin-like peptides. Co-incubation of prolactin and placental lactogen with plasmin was performed and analyzed by gel electrophoresis and Western blotting. Mass spectrometric analyses were carried out for sequence validation and precise cleavage site identification. The cleavage sites responsible for the generation of the vasoinhibin-like peptides were located at K170-E171 in prolactin and R160-T161 in placental lactogen. Various genetic variants of the human prolactin and placental lactogen genes are projected to affect proteolytic generation of the vasoinhibin-like peptides. The endogenous counterparts of the vasoinhibin-like peptides generated by plasmin may represent vasoinhibin-isoforms with inhibitory effects on vasculature and coagulation.

1. Introduction

Vasoinhibin is a peptide hormone with a diverse array of endocrine, paracrine, and autocrine effects, ranging from the regulation of blood vessel growth, permeability, and dilation (Clapp et al., 2015) to non-vascular effects, which include the stimulation of vasopressin release (Mejia et al., 2003), the stimulation of anxiety- and depression-related behavior (Zamorano et al., 2014), and thrombolytic effects (Bajou et al., 2014). Vasoinhibin has been investigated in the context of several human diseases, and pathophysiological roles emerged in vasoproliferative retinopathies (Arnold et al., 2010; Triebel et al., 2009, 2011) and pregnancy-associated diseases (Hilfiker-Kleiner et al., 2007; Nakajima et al., 2015; Gonzalez et al., 2007; Leanos-Miranda et al., 2008), including its evaluation in clinical interventional studies (Hilfiker-Kleiner et al., 2017; Robles-Osorio et al., 2018).

Vasoinhibin-isoforms are generated by the proteolytic cleavage of their precursor molecules prolactin (PRL),[2] growth hormone (GH), and placental lactogen (PL) (Struman et al., 1999; Corbacho et al., 2002). Vasoinhibin can be generated in various anatomical compartments or tissues, including the pituitary gland (Cruz-Soto et al., 2009; Sinha et al., 1987), the placenta (Struman et al., 1999; Perimenis et al., 2014), the retina (Aranda et al., 2005) the mammary gland (Ishida et al., 2014), the heart (Hilfiker-Kleiner et al., 2007) and cartilage (Macotela et al., 2006). Vasoinhibin-generating enzymes include cathepsin D, matrix metalloproteinases and bone morphogenetic protein 1 (Struman et al., 1999; Corbacho et al., 2002; Macotela et al., 2006; Piwnica et al., 2004; Ge et al., 2007). Depending on the cleavage site vasoinhibin varies in size, and isoforms ranging from 9 to 18 kDa have been reported (Macotela et al., 2006; Piwnica et al., 2004; Ge et al., 2007). The investigation of the generation of vasoinhibin by cleavage of PRL and PL is important, as the identification of vasoinhibin-isoforms is not completed, nor is the list of enzymes capable of generating them. The regulation of vasoinhibin is embedded into an endocrine axis named the prolactin/vasoinhibin axis, featuring tiers of control at the hypothalamic, the pituitary and the

* Corresponding author. Institute for Clinical Chemistry, Laboratory Medicine and Transfusion Medicine, Nuremberg General Hospital & Paracelsus Medical University, Prof.-Ernst-Nathan-Str. 1, 90419, Nuremberg, Germany.
E-mail address: Jakob.Triebel@gmx.de (J. Triebel).

[1] equal contribution & first authorship.
[2] Prolactin = PRL, growth hormone = GH, placental lactogen = PL.

https://doi.org/10.1016/j.mce.2021.111471
Received 28 June 2021; Received in revised form 16 September 2021; Accepted 29 September 2021
Available online 1 October 2021

peripheral level (Triebel et al., 2015). The discovery of enzymes capable of releasing vasoinhibin by cleaving their precursors PRL, GH, and PL, as well as the precise location of the cleavage sites will help to better understand this hormonal axis and its role in health and disease. Specifically, elucidation of the generation of vasoinhibin from PL may help clarify the contribution of lactogenic hormones to pregnancy diseases characterized by endothelial cell dysfunction, such as preeclampsia (Lenke et al., 2019). The cleavage of growth hormone by the peptidase plasmin (EC 3.4.21.7) has been reported (Li and Graf, 1974), and plasmin is known for its effects in fibrinolysis and thrombolysis. Vasoinhibin, in turn, inhibits the antifibrinolytic activity of plasminogen activator inhibitor-1 (PAI-1), protected mice against thromboembolism and promoted arterial clot lysis (Bajou et al., 2014). In this context, plasmin appears as an enzyme which may be capable of vasoinhibin generation and therefore an adequate subject of investigation.

2. Materials and methods

Reagents. Recombinant human PRL expressed in HEK cells (cat. no. SRP9000) and purified human PL from human placental tissue (cat. no. PHP157G) were purchased from Sigma-Aldrich and Bio-Rad, respectively. Natural human plasmin (cat. no. ab90928) was purchased from Abcam. Antibodies against PRL and PL as well as their immunogens and epitope regions are listed in Table 1. Horseradish peroxidase-conjugated secondary antibodies against rabbit IgG (HRP-goat anti-rabbit IgG (1:3000), code 111-035-045) or mouse IgG (HRP-goat anti-mouse IgG (1:3000), code 115-035-062) from Jackson ImmunoResearch Laboratories Inc. (West Grove, PA, USA) were used to detect and visualize the primary antibodies.

Cleavage of PRL/PL with plasmin. 250 ng of PRL or 1 μg PL were incubated with 100 ng or 1.34 μg, respectively, of plasmin in a final volume of 13 μl of 0.1 M Tris base buffer (pH 7.4). The incubations were carried out in a thermoblock at 37 °C for time periods ranging from 10 to 360 min. PRL, PL, and plasmin were also incubated separately under the same conditions. All time periods represented end-point incubations.

SDS-PAGE and Western blotting. The incubated samples were subjected to SDS-PAGE using a Bio-Rad Mini-Protean Cell with 4–20% SDS stain-free precast gels (Bio-Rad, cat. no. 456–8093). The molecular weight Precision Plus Protein Western C Standard (Bio-Rad cat. no. 161–0376) was used. Electrophoresis was performed at 200 V for approximately 30 min. After electrophoresis, a gel total protein image using the Stain Free technology with UV-light activation was obtained using the Chemi Doc MP Imaging System (Bio-Rad, cat. no. 170–8280). The proteins were transferred onto PVDF membranes, pore size 0.2 μm (Bio-Rad, cat. no. 1704272) with the Bio-Rad Tran-Blot Turbo Transfer System (cat. no. 170–4155) at 25 V and 1.4 A for 7 min. The membranes were blocked by incubation with 50 ml of 4% dry milk in TBST (0.1% Tween 20) at RT for 1 h on an orbital shaker. Each membrane was incubated with the respective primary antibody overnight at 4 °C under rotation. The membranes were washed and incubated with the secondary antibody for 3 h, at RT under rotation. After repeated washing, the antigen-antibody complex was detected by incubation of the membranes with 6 ml of a development solution (Pierce ECL Western blotting Substrate, Waltham, Massachusetts, USA, cat. no. 32209) for 1 min. Chemiluminescence images were obtained using the Chemi Doc MP Imaging System. Observed molecular weights were determined with Image Lab (Bio-Rad, version 5.2.1, 2014), theoretical molecular weights were calculated using ExPASy (Artimo et al., 2012).

Mass spectrometry (MS). MS analyses of 16.1 kDa PRL and 15.7 kDa PL were performed at Proteome Factory Berlin. Briefly, an in gel enzymatic cleavage was performed in which the gel bands were prepared for enzymatic cleavage by their swelling and shrinking 3 times in 100 mM TEAB and 50 mM TEAB, and 60% acetonitrile, respectively. During consecutive swelling steps the bands were treated with TCEP (5 mM final) and IAA (10 mM final) for reduction and alkylation of cysteine residues. Each step was carried out for 20 min at RT. After the last shrinking step, the gel slices were dried in open Eppendorf cups for 15 min. Subsequently the samples were digested separately by endoproteases (trypsin, chymotrypsin, elastase, LysC, ALM; with an enzyme amount of 200 ng). *High-resolution MS:* The Agilent 1100 nanoLC system was coupled to an Orbitrap XL mass spectrometer (ThermoFisher, Bremen, Germany). Samples from proteolysis were applied to nanoLC-ESI-MS/MS after acidification. After trapping and desalting the peptides on enrichment column (Zorbax SB C18, 0.3 mm × 5 mm, Agilent) using 0.5% acetonitrile/0.5% formic acid solution for 5 min peptides were separated on Zorbax 300 SB C18, 75 μm × 150 mm column (Agilent, Waldbronn) using an acetonitrile/0.1% formic acid gradient of 5%–40% acetonitrile. MS overview spectra were automatically taken in FT-mode according to manufacturer's instrument settings for nanoLC-ESI-MS/MS analyses. Peptide fragmentation (CID) and detection operated in iontrap-mode. *Database searches:* Data sets acquired by MS were used for database searches. The search parameters were set according to the

Table 1
Western blotting and mass spectrometic features of plasmin mediated cleavage-products of human prolactin and placental lactogen. A combination of antibody epitopes and/or their known immunizing peptide sequences, Western blotting, observed and calculated molecular masses, as well as mass spectrometry was used to establish the cleavage sites.

Antibodies			Western Blots		Calc. Weight	Mass Spectrometry	
Antibody	Immunogen	Epitope	WB Figure	Reactive bands, cleavage products	with cleavage at indicated site	MS sequences	LCMS area over peptide start
Prolactin							
ABIN1500431, Antibodies online, mouse monoclonal ab	Full-length recombinant protein of human PRL produced in HEK293T cell	PRL +++ Vi – (C-term)	Fig. 1B & 1.D	16.1 kDa +++	K81-A82: 16.861 kDa	Band at 16.1 kDa: AA 82–215	–
				6.8 kDa +++	K170-E171: 6.791 kDa		
ab92489, Abcam, rabbit monoclonal	synthetic peptide corresponding to residues in human PRL	PRL +++ Vi ++ (N-term)	Fig. 1C	16.1 kDa +	K170-E171: 16.124		–
				6.8 kDa +	K81-A82: 6.054 kDa		
Placental lactogen							
ABIN1881233, Antibodies online, rabbit polyclonal	Synthetic peptide generated with a KLH conjugated peptide of AA 42–70 of PL	Full-length PL and N-term fragments	Fig. 4B & 4.C	15.7 kDa +++	R160-T161: 15.687 kDa	Band at 15 kDa: AA 27-217	Major N-term variant: VQTVPLSR , 99.84%
				9 kDa ++ (PL std.)	triple L motif: 9.459 kDa		
ABIN6544883, Antibodies online, rabbit polyclonal	Synthetic peptide generated with a KLH conjugated peptide of AA 177–204 of PL	Full-length PL and C-term fragments	Fig. 4D	15 kDa +	S81-D82: 15.805 kDa		Major C-term variant: DLEEGIQTLMGRLEDGSRR (142–160), 98.1%

expected protein modifications and to the MS instrument used in this study. Sequence assembly was accomplished by PEAKS (Bioinformatics solutions) software with respect to the given enzyme specificities. In peptide mapping possible amino acid modifications were set to oxidation (at methionine), carbamidomethylation (at cysteines) and deamidation (asparagine → aspartate).

Genetic variant analysis of the PRL and the PL cleavage sites. Human PRL and PL transcripts PRL-201 and CSH1-201 (placental lactogen), respectively, were reviewed in ENSEMBL (Zerbino et al., 2018). Based on the MEROPS (Rawlings et al., 2018) entry for plasmin (entry S01.233), a score indicating the cleavage efficiency for each cleavage site was calculated as published previously ((Triebel et al., 2019; Triebel et al., 2017a). Briefly, the number of observed cleavages with an amino acid on a particular position in the cleavage site was retrieved from the MEROPS specificity matrix for plasmin and added with the other numbers for each position to generate a score for the wt sequence of the cleavage site (8P-score). The designations P1, P2, P3 and P4 are the amino acids towards the N-terminus and P1′, P2′, P3′, and P4′ are towards the C-terminus and the cleavage occurs between P1 and P1'. The effect of genetic variants was expressed by the difference of the 8P-score compared to the score for the wt sequence.

Amino acid position numbering. All amino acid position numbers of the sequences were denoted in accordance with their UniProt entries, which starts numbering with the first amino acid of the signal peptide. To avoid a possible source of misinterpretation, the amino acid positions of the cleavage sites when starting the numbering at position 1 of the mature protein were also indicated in brackets.

3. Results

Plasmin generates 16.1 and 6.8 kDa fragments from PRL. Incubation of PRL with plasmin for 10 min and subsequent analysis with SDS-PAGE demonstrates the generation of two fragments with 16.1 and 6.8 kDa molecular masses, respectively (Fig. 1A). The uncleaved fraction of PRL, as well as the 16.1 and the 6.8 kDa PRL-fragments were immunoreactive to a mouse monoclonal antibody raised against full-length PRL with a C-terminal epitope (Fig. 1B). The uncleaved PRL, the 16.1 kDa and 6.8 kDa fragment were also reactive when probed with a rabbit monoclonal antibody directed against an N-terminal epitope of PRL (Fig. 1C). Incubation of PRL with plasmin from 10 to 360 min and Western blotting with an anti-N-terminal PRL antibody demonstrated that both the intensity of the PRL band as well as the intensity of the 16.1 kDa band decreased with time (Fig. 1D). A sequence coverage map derived from a non-directed nanoLC-ESI-MS/MS showed multiple peptide detections starting from position 81 until lysine in position 170, whereas a relatively low coverage was present for the positions of

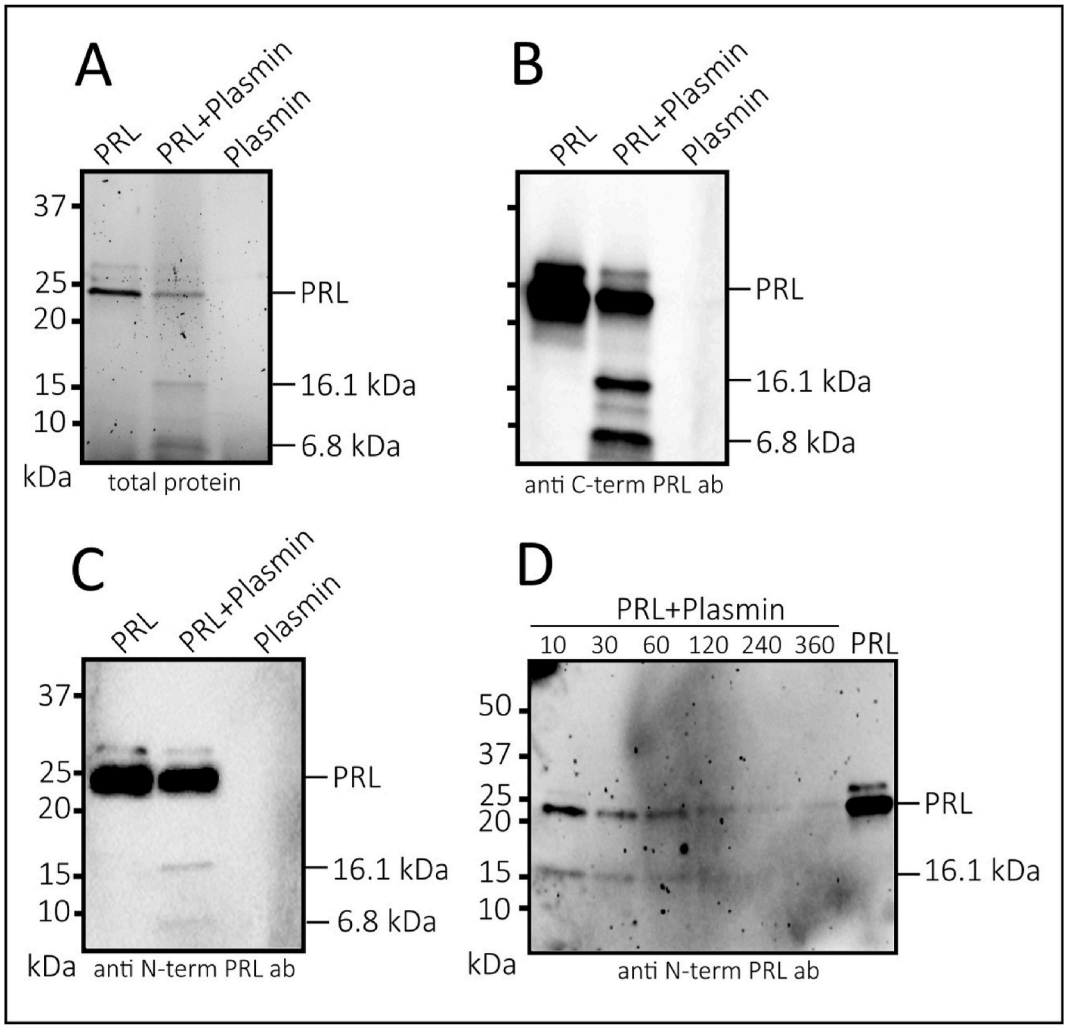

Fig. 1. Cleavage of PRL by plasmin. (A) Total protein in SDS-gel. Apart from uncleaved PRL, 16.1 and 6.8 kDa bands are visible. (B) Western blot with anti-C-term PRL antibody (ABIN1500431) demonstrates the high abundance of C-terminal fragments at 16.1 and 6.8 kDa. (C) Western blot with anti N-term PRL antibody (ab92489) demonstrates a relatively low abundance of N-terminal fragments at 16.1 and 6.8 kDa. (D) Plasmin incubation timeline (10–360 min), Western blot with anti N-term PRL antibody (ab92489) demonstrates that both, full-length PRL and the vasoinhibin-like, N-terminal PRL fragment degrade with time.

glutamic acid at 171 and beyond (Fig. 2A/B). Based on the match between the observed and calculated molecular masses, the antibody reactivity in Western blotting, and the peptides detected by MS, it was concluded that the bands at 16.1 and 6.8 kDa contained a mixture of fragments with N- and C-terminal PRL sequences (Table 1). A 16.1 kDa C-terminal fragment was apparently generated by cleavage at K81-A82 (K53-A54), while an N-terminal 16.1 kDa fragment was generated by cleavage at K170-E171 (K142-E143) and an absent cleavage at K81-A82. Both, cleavage at K81-A82 and K170-E171, generated a 6.8 kDa N-terminal fragment and a 6.8 kDa C-terminal fragment, respectively (Fig. 1B/C).

To substantiate the presence of an N-terminal PRL sequence in the 16.1 kDa band, as indicated by its reactivity with the anti N-term PRL antibody but put into question by absence of MS peptide detections, multiple replications of this band were excised and subjected to nanoLC-ESI-MS/MS. A directed search for the calculated m/z-value of the proposed peptide LPICPGGAAR, corresponding to the amino acid positions 29–38 of PRL (positions 1–28 correspond to the signal peptide not present in mature PRL), was performed and the resulting fragment mass spectrum/fragment ion map confirmed the presence of this peptide in

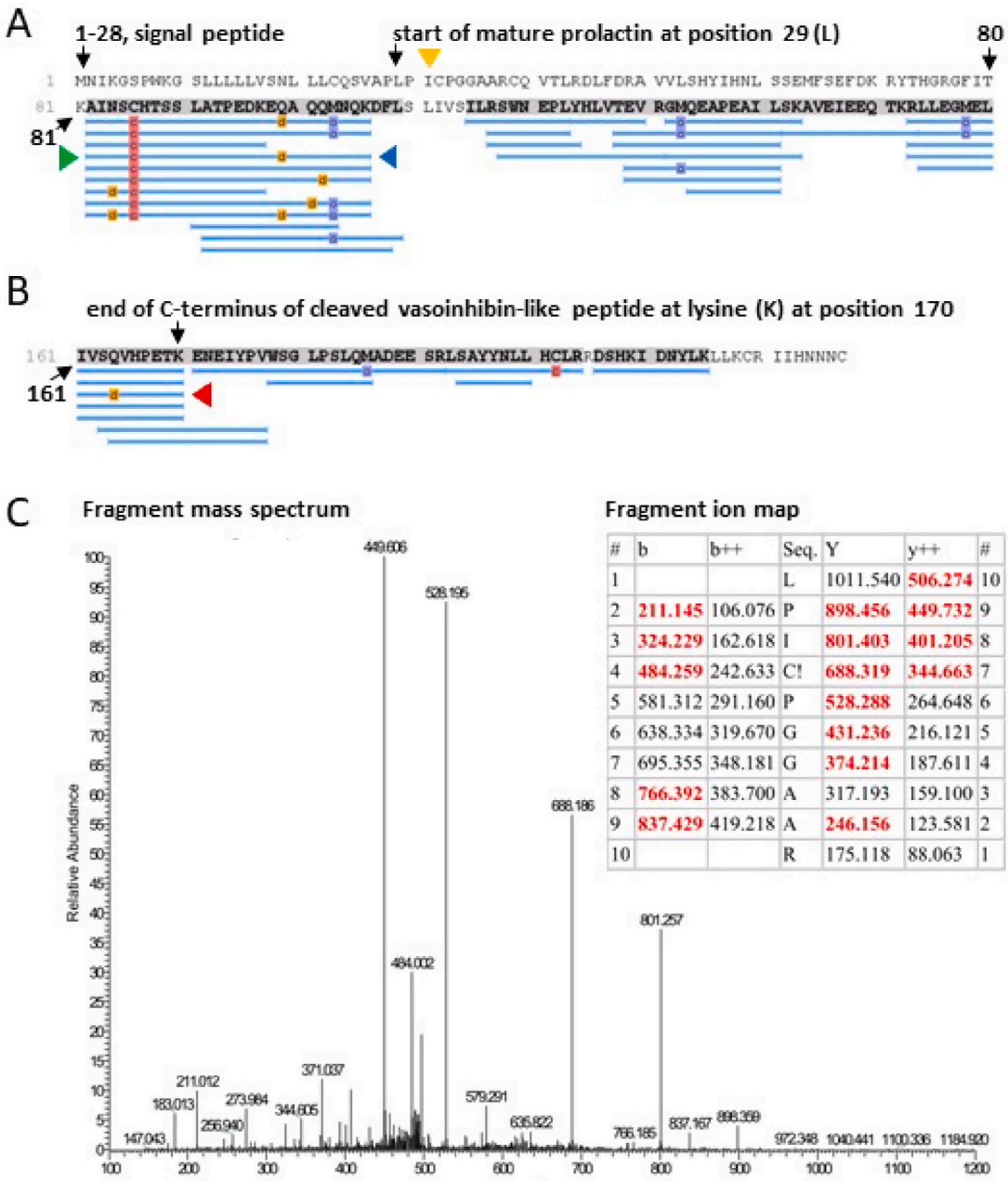

#	b	b++	Seq.	Y	y++	#
1			L	1011.540	506.274	10
2	211.145	106.076	P	898.456	449.732	9
3	324.229	162.618	I	801.403	401.205	8
4	484.259	242.633	C!	688.319	344.663	7
5	581.312	291.160	P	528.288	264.648	6
6	638.334	319.670	G	431.236	216.121	5
7	695.355	348.181	G	374.214	187.611	4
8	766.392	383.700	A	317.193	159.100	3
9	837.429	419.218	A	246.156	123.581	2
10			R	175.118	88.063	1

Fig. 2. PRL peptide coverage map of the 16.1 kDa band generated by plasmin. Modified residues are highlighted in different colors with respect to their identity (red = carbamidomethylation, yellow = deamidation, blue = oxidation). Leucing/Isoleucine residues are isobaric and therefore not discriminable in MS. A) Large portions of the PRL sequence starting at position 82 are covered, consistent with the Western blot analysis showing the high abundance of C-terminal fragments in the cleavage products. The high abundance of peptides starting at position 82 (green arrow), demonstrates cleavage between position 81 and 82. B) Multiple peptides ending at position 170 (red arrow) indicate cleavage between position 170-and 171. C) Fragment mass spectrum and fragment ion map to validate the presence of the N-terminal PRL sequence LPICPGGAAR (yellow arrow in A)). Further cleavage sites could be assumed on the basis of the peptide coverage maps, such as K106-D107 (A, blue arrow), however, they were disregarded since no corresponding fragment was detected by SDS-PAGE/WB. (For interpretation of the references to color in this figure legend, the reader is referred to the Web version of this article.)

the band (Fig. 2C). The calculated molecular mass of an N-terminal PRL fragment comprising amino acids 29–170 is 16.1 kDa and consistent with the apparent mass of 16.1 kDa observed in the electrophoresis.

The immunoreactivity of the 16.1 kDa band to an anti N-terminal PRL antibody and the presence of the first 9 N-terminal amino acids of PRL, together with the sequence coverage derived from MS analysis, identified a minor fraction in the band as a vasoinhibin-like peptide, comprising amino acids 29–170, with a novel cleavage site for plasmin between the amino acids K170-E171 (K142-E143) (Fig. 3). In the three-dimensional structure of PRL, the cleavage site projected into L3, a region which is typical for the generation of vasoinhibin by various other proteases, for example cathepsin D and matrix metalloproteases. Western blotting of the cleavage products showed that a C-terminal fragment was the major fragment generated (Fig. 1B) and that the N-terminal fragment was a minor fraction (Fig. 1C) and had little stability when subjected to longer incubation ranging from 30 to 360 min (Fig. 1D).

Generation of 15.7 kDa PL-fragments. PL cleavage by plasmin generated a 15.7 kDa fragment (Fig. 4 A), which was detected by an anti-N-terminal PL antibody (Fig. 4B) by Western blotting. When PL was incubated with plasmin at 37 °C, for a period between 10 and 360 min and analyzed by Western blotting, the intensity of the PL bands decreased continuously and the intensity of the resulting N-terminal 15.7 kDa PL-fragment increased proportionately (Fig. 4C). The same analysis using an anti-C-terminal PL antibody demonstrated a gradual decrease of both, full-length PL and a 15.7 kDa C-terminal PL-fragment (Fig. 4D). Comparable to PRL, it was concluded that the band at 15.7 kDa contained a mixture of fragments with N- and C-terminal PL sequences. For precise identification of the cleavage site, the band was sequenced by nanoLC-ESI-MS/MS and a sequence coverage map was created (Fig. 5). Also, the LCMS area over the peptide start position was analyzed. The major N-terminal variant started at position 27 with VQTVPLSR (Fig. 5A) and the major C-terminal variant ended with the sequence DLEEGIQTLMGRLEDGSRR at position 160 (Fig. 5B). Their relative sum percentages of the area over the peptide start position was 99.84% and 98.1%, respectively (Table 1). Thus, cleavage of PL by plasmin generating the N-terminal fragment occurred between the amino acids R160-T161 (R134-T135) (Fig. 6). Calculation of the molecular weight of the N-terminal PL fragment comprising AA 27–160 resulted in 15.687 kDa, which is close to the mass of 15.7 kDa observed in SDS-PAGE (Table 1). The PL cleavage site was located in the loop connecting the third and fourth α-helixes at position R160-T161 (R134-T135) (Fig. 6). Western blotting (Fig. 4C and D) and the LCMS area over peptide start position (Table 1) showed that the N-terminal fragment is the major fraction in the 15.7 kDa band and that had high stability when subjected to longer incubation (Fig. 4C). The C-terminal fragment as well as full-length PL disappeared with longer incubation times (Fig. 4D). In agreement with the Western blot (Fig. 4D), the MS peptide coverage map (Fig. 5), and the calculated molecular mass (Table 1), the C-terminal fragment most likely arose from cleavage at S81-D82 (S55-D56). A 9 kDa fragment was observed in the total protein staining of PL and in Western blots of the PL-standard when the membranes were probed with an anti N-term PL antibody (Fig. 4A, B and C). This 9 kDa fragment was not detected in Western blotting of PL after incubation with plasmin (Fig. 4B and C), but is consistent with cleavage in the triple L motif of the PL sequence at positions 106–108 (81–83) (Fig. 5B, purple arrow). A 38 kDa band was observed in the Western blot of the PL with an anti C-term antibody (Fig. 4D). This band may correspond to a PL aggregate or may be unspecific.

Genetic variant analysis of the PRL K170-E171 (K142-E143) and the PL R160-T161 (R134-T135) cleavage sites. A genetic variant analysis of the PRL K170-E171 and the PL R160-T161 cleavage sites showed that multiple point mutations and inframe deletions have been found in the cleavage site (Tables 2 and 3). Some of the variants highly likely affect proteolytic cleavage, while others appear to have only little effect. For example, the point mutation in PRL at P4' which leads to an Ile > Val substitution is likely to have little to no effect (8P score −1), while the inframe deletion affecting 5 of the 8 relevant amino acid residues in the cleavage site, including the important residue lysine at P1', is likely to abolish cleavage by plasmin at this site (Table 2). Similarly, the PL cleavage site is likely affected by multiple genetic variants either enhancing or inhibiting cleavage by plasmin. For example, the replacement of arginine in P2 may facilitate cleavage (8P-score +9), while Arg > Trp likely abolishes cleavage at this site, as no experimentally observed cleavage by plasmin with tryptophane in P1 is listed in the MEROPS database (8P-score −65, Table 3).

4. Discussion

The present study identifies plasmin as a protease able to cleave PRL and PL. The resulting cleavage products are a mixture of fragments of 15 and 16 kDa masses containing N- and C-terminal portions of the uncleaved molecules. Biological functions of the C-terminal fragments are unknown. The 15 and 16 kDa N-terminal fragments, however, most likely constitute vasoinhibin isoforms with their typical biological effects, as the first 79 amino acids comprising the vasoinhibin anti-angiogenic domain (Robles et al., 2018) are present. However, the biological effects were not tested in this study, which is a limitation. Both, PRL and PL, are susceptible to cleavage by plasmin in their L1 and L3-regions. In PRL, the cleavage site in L1 appears to be preferentially used compared to that in L3, as the major species is a C-terminal 16 kDa fragment. The N-terminal 16 kDa fragment was of little stability when subjected to longer incubation, which may indicate short term biological

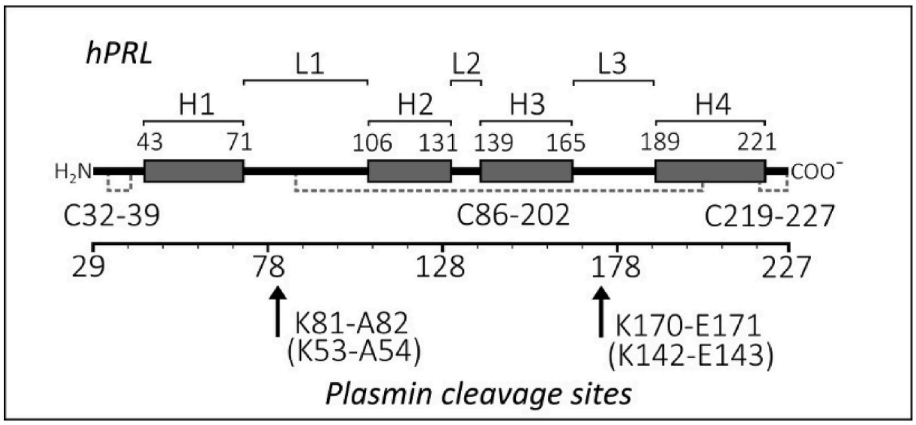

Fig. 3. (A) Human full-length PRL schematics with alpha-helices (H1-4), loops (L1-3), disulfide bonds and their corresponding amino acid positions. The plasmin cleavage sites are as determined by mass spectrometry are located in L1 (between lysine at position 81 and alanine at position 82) and L3 (between lysine at position 170 and glutamine at position 171). The numbers in brackets indicate amino acid positions starting from the first residue after the signal peptide.

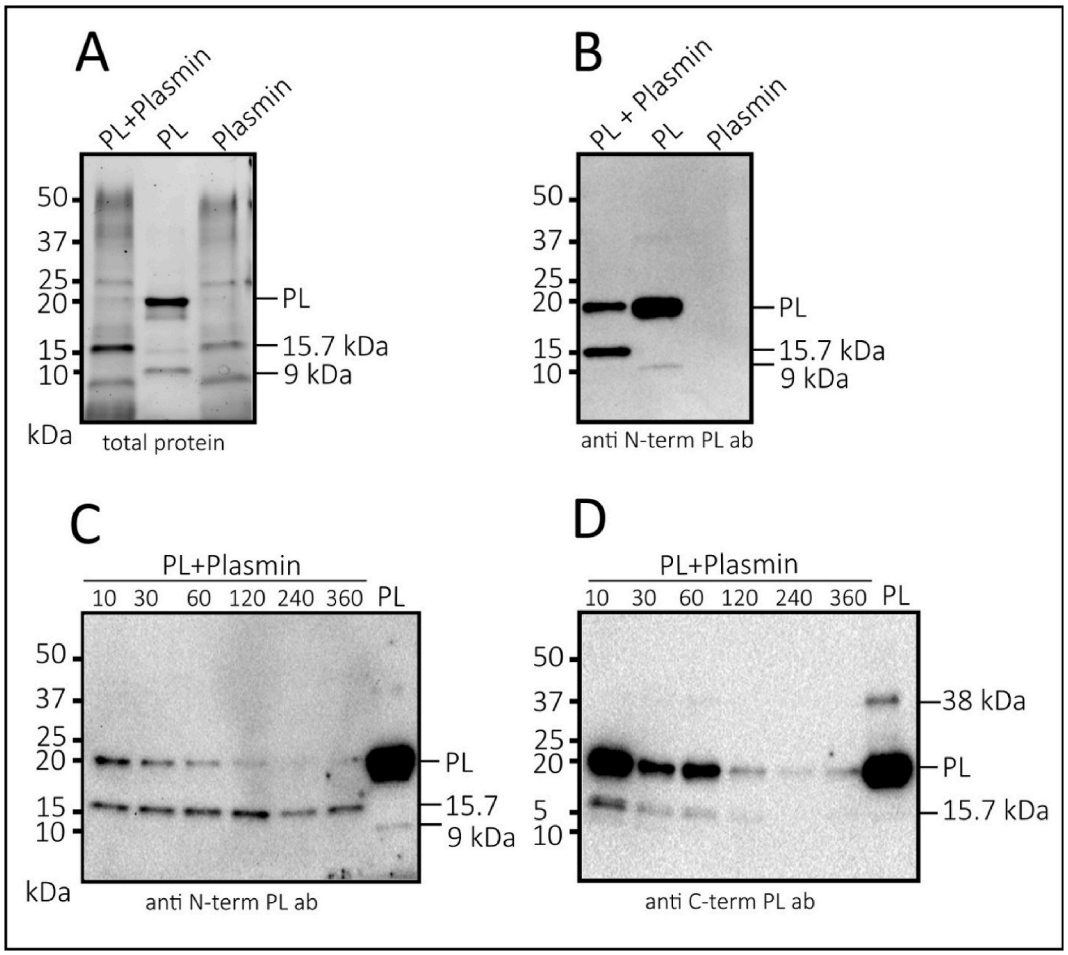

Fig. 4. Cleavage of PL by plasmin. (A) Total protein in SDS-gel. 15.7 and 9 kDa bands are visible. (B) Western blot incubation with anti N-term PL antibody ABIN1881233 demonstrates a high abundance 15.7 kDa N-terminal, vasoinhibin-like peptide. A 9 kDa, N-terminal PL fragment is seen in the PL standard. (C) Plasmin incubation timeline (10–360 min), Western blot with anti N-term PL antibody ABIN1881233 demonstrates degradation of full-length PL with time, but stability of the 15.7 kDa N-terminal, vasoinhibin-like peptide. (D) Incubation timeline (10–360 min), Western blot with anti C-term PL antibody ABIN6544883 demonstrates the presence of a low abundance, C-terminal PL fragment which degrades with time.

effects or limited physiological significance. In PL, the cleavage site in L3 is preferentially used, as the major species is an N-terminal 15 kDa fragment. The 15 kDa fragment is stable over time, even more stable than full-length PL, and does not seem to be further cleaved at the L1 site which is used by plasmin in full-length PL. The small 6.8 kDa N-terminal PRL fragment emerging from cleavage in L1 may also constitute a vasoinhibin isoform. Cleavage at lysine (K) and arginine (R) at position 1 (P1) of the cleavage site is consistent with the cleavage profile of plasmin previously reported and shown by PROSPER (Cao et al., 1999; Song et al., 2012). Except the cleavage sites indicated in Figs. 3 and 6, other cleavage sites can be derived from the sequence coverage maps, such as a likely site in PRL at K106-D107 (Fig. 2A, blue arrow). However, the present study focused only on cleavage sites for which the corresponding peptides were detected by SDS-PAGE/WB, which was not the case for K106-D107 (it may also be an artifact due to enzymatic digestion during the sample preparation). PRL is also cleaved by cathepsin D and matrix metalloproteases, and a relevant consideration is the comparison of the cleavage efficiency of these enzymes with plasmin. This should be determined experimentally, however, an estimation is possible by comparing the 8P-scores. The 16.8 kDa vasoinhibin isoform generated by cathepsin D demonstrates an 8P-score of 409, and the 17.7 kDa vasoinhibin isoform generated by matrix metalloprotease 8 and 13 demonstrates 8P-scores of 120 and 159, respectively (Triebel et al., 2017a). The 8P-scores for the 16.1 kDa vasoinhibin-like peptide from PRL is 109 (Table 2). This indicates that the cleavage efficiency of plasmin-mediated vasoinhibin generation is likely lower than that of cathepsin D, but possibly on the same level with matrix metalloproteases.

The cleavage of growth hormone by plasmin has been reported by Li et al., however the resulting N-terminal fragment has not been investigated for vasoinhibin-like bioactivity (Li and Graf, 1974). Plasmin is a serine endopeptidase which is activated by cleavage of plasminogen and stimulates fibrinolysis. The initiation of cleavage of the proenzyme plasminogen occurs via tissue plasminogen activator (tPA) and by urokinase-type plasminogen activator (uPA) which are inhibited by PAI-1. Both, uPA and PAI-1 have been described as binding partners of vasoinhibin and vasoinhibin inhibited the antifibrinolytic activity of PAI-1 (Bajou et al., 2014). Vasoinhibin generated by plasmin may therefore function as a downstream mediator of fibrinolytic plasmin effects. The molecular mass of the vasoinhibin isoform which is generated by plasmin-mediated cleavage of PRL shown here is consistent with reported detections of PRL-derived vasoinhibin (16 kDa) (Duenas et al., 2004). A vasoinhibin-like peptide similar to that derived from PL, however, has not been previously reported. PL-derived vasoinhibin is of particular interest in pregnancy-associated diseases, such a preeclampsia and peripartum cardiomyopathy. An involvement of vasoinhibin has been reported for both diseases, but the focus was PRL-derived vasoinhibin and the possibility of PL-derived vasoinhibin isoforms was disregarded (Hilfiker-Kleiner et al., 2007; Gonzalez et al., 2007). Vasoinhibin may also be involved in postpartum depression (Triebel

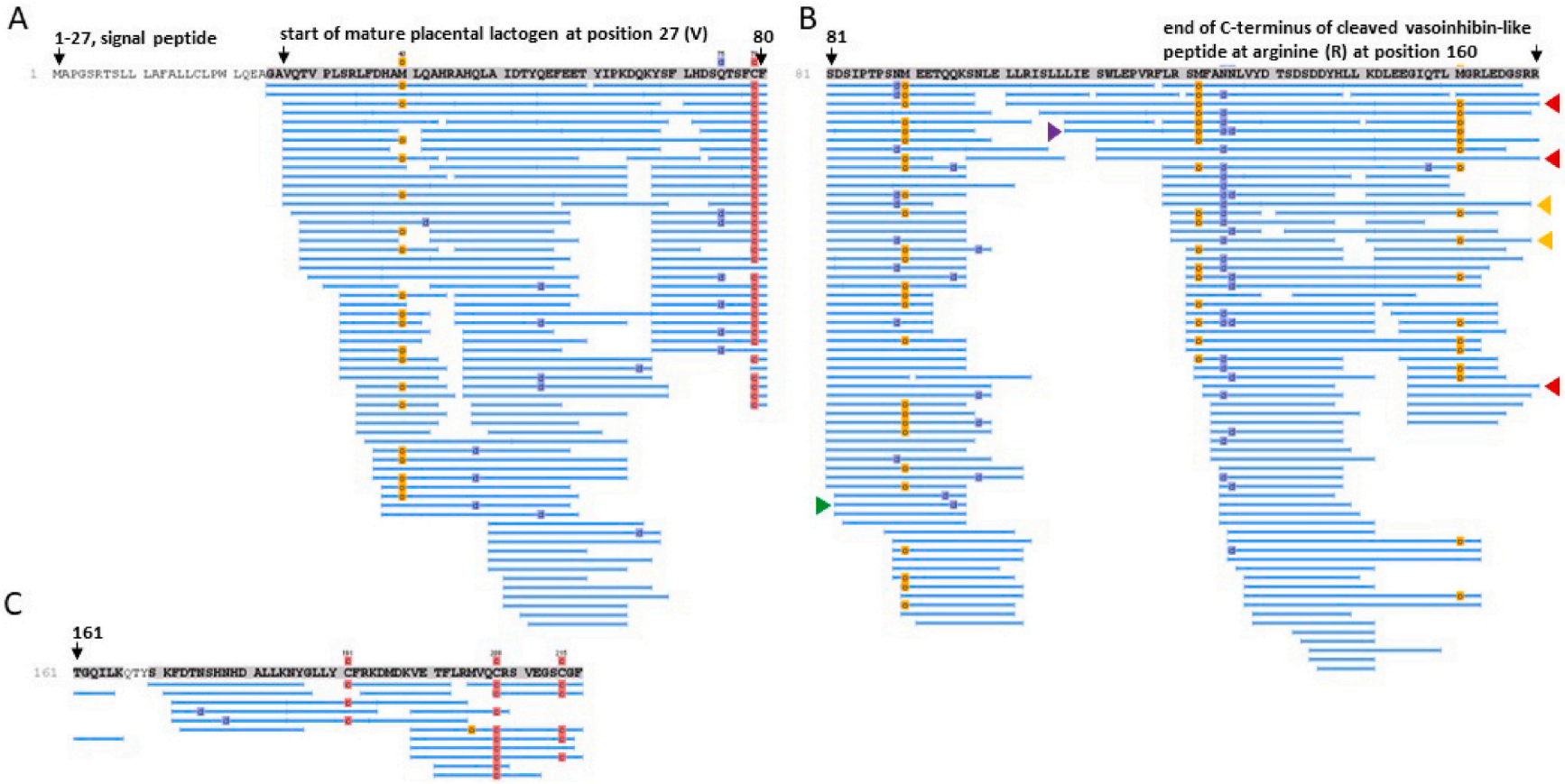

Fig. 5. A, B and C. PL Peptide coverage map of the 15.7 kDa band generated by plasmin. Large portions of the PL sequence starting 27 (valine) are covered. Multiple peptides ending with arginine at position 160 (red arrows in part B) or arginine at position 159 (part B, yellow arrows) were detected, indicating cleavage between arginine at position 160 and threonine at position 161. Further, multiple peptides starting with asparagine at position 82 are detected (part B, green arrow), indicating cleavage between serine at position 81 and asparagine at position 82. The peptides starting with residues LIE (part B, purple arrow) indicate cleavage within the triple L motif, which could explain the 9 kDa band present in the purified human PL standard preparation. (For interpretation of the references to color in this figure legend, the reader is referred to the Web version of this article.)

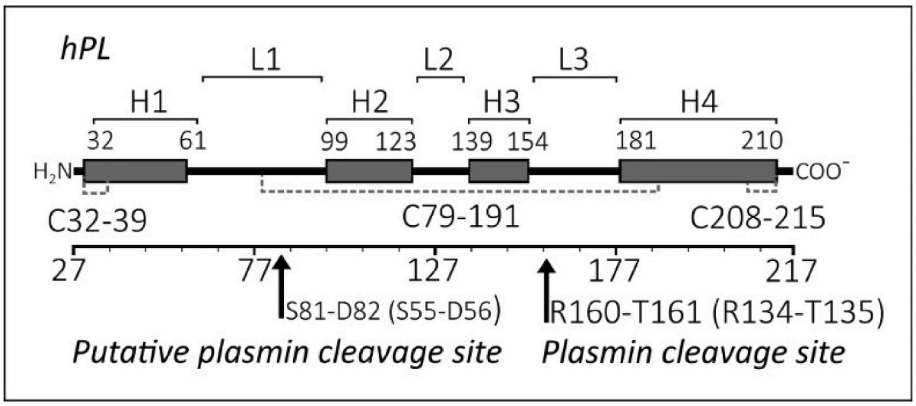

Fig. 6. (A) human full-length PL schematics with alpha-helices (H1-4), loops (L1-3), disulfide bonds and their corresponding amino acid positions. The plasmin cleavage sites as determined by mass spectrometry are located in L1 (putative cleavage site at serine in position 81 and asparagine in position 82) and L3 (between arginine at position 160 and threonine at position 161). The numbers in brackets indicate amino acid positions starting from the first residue after the signal peptide.

Table 2
Genetic variant analysis of a cleavage site in PRL. Cleavage-site of the 16.1 kDa vasoinhibin-like peptide generated by plasmin by cleavage of PRL between lysine in position 170 and glutamine in position 171 with adjacent amino acids. The numbers below the amino acids indicate observed cleavages with the amino acid at the corresponding position in the cleavage site, retrieved from the MEROPS-database. Cleavage occurs between P1 and P1', indicated by the red line. The 8P-score, indicating cleavage efficiency, is 109 in the wt-sequence but varies with the indicated point mutations or inframe deletions in the cleavage site, which were retrieved from reviewing ENSEMBL on the PRL transcript PRL-201. A lower score than 109 indicates a lower cleavage efficiency, and a higher score a higher cleavage efficiency.

Vi-isoform	Enzyme/Subst.	Amino acid position/P-position/Amino acid/number of observed cleavages (MEROPS)								8P-score	8P-change
16.1 kDa Vasoinhibin-like peptide (from PRL)		167	168	169	170	171	172	173	174		
		P4	P3	P2	P1	P1′	P2′	P3′	P4′		
		Pro	Glu	Thr	Lys	Glu	Asn	Glu	Ile		
	Plasmin	18	7	3	57	3	7	7	7	109	
	Pro > Leu	P4	P3	P2	P1	P1′	P2′	P3′	P4′		
	rs749070148	Leu	Glu	Thr	Lys	Glu	Asn	Glu	Ile		
	Plasmin	7	7	3	57	3	7	7	7	98	−11
	Pro > Thr	P4	P3	P2	P1	P1′	P2′	P3′	P4′		
	rs1284955612	Thr	Glu	Thr	Lys	Glu	Asn	Glu	Ile		
	Plasmin	5	7	3	57	3	7	7	7	96	−13
	Asn > Ser	P4	P3	P2	P1	P1′	P2′	P3′	P4′		
	rs1370241165	Pro	Glu	Thr	Lys	Glu	Ser	Glu	Ile		
	Plasmin	18	7	3	57	3	12	7	7	114	5
	Ile > Val	P4	P3	P2	P1	P1′	P2′	P3′	P4′		
	rs1472067934	Pro	Glu	Thr	Lys	Glu	Asn	Glu	Val		
	Plasmin	18	7	3	57	3	7	7	6	108	−1
	inframe deletion	P4	P3	P2	P1	P1′	P2′	P3′	P4′		
	rs1401537723	Pro	Glu	Thr	Glu	Ile	Tyr	Pro	Val		
	Plasmin	18	7	3	1	4	5	11	6	55	−54

et al., 2017b). The vasoinhibin-like peptides generated by plasmin shown here may have endogenous counterparts with effects on vasculature, fibrinolysis, and anxiety behavior.

The genetic variant analysis of the PRL K170-E171 (K142-E143) and the PL R160-T161 (R134-T135) cleavage sites demonstrates that point mutations or other genetic variants with an effect on the sequence within the 8 amino acid cleavage sites can inhibit or facilitate proteolytic cleavage and thus vasoinhibin generation. Clinical information about the patients in which these mutations were found were not available in the database, hence no studies of phenotypes or related pathologies could be executed. It is suggested that genetic variants affecting vasoinhibin generation may be protective or aggravating factors in vascular diseases, diabetic retinopathy, preeclampsia, or peripartum cardiomyopathy. More resolute sequencing of PRL and PL genes in these patients will show whether this assumption can be consolidated or refuted.

The growing list of proteases able to generate vasoinhibin relates to general questions. How does generation by multiple proteases fit with the concept of specificity in classical endocrinology? It is evident that the bioactive, antiangiogenic domain of vasoinhibin is preserved in a variety of isoforms generated by the various proteases as long as at least the first 79 amino acids of the PRL precursor sequence are conserved (Robles et al., 2018). The bioactive domain of the various vasoinhibin isoforms interacts with soluble binding partners and/or cell surface binding sites to mediate its effects on target tissues, such as the endothelium (Bajou et al., 2014; Clapp and Weiner, 1992; Morohoshi et al., 2018). Thus, despite its posttranslational generation - as opposed to the cellular expression and secretion of peptide hormones with non-variable sequence lengths – vasoinhibin is specific to it's binding partners by conservation of its bioactive domain. Moreover, the high conservation of cleavage sites across species supports the concept of specificity (Macotela et al., 2006; Triebel et al., 2015).

How is generation by multiple proteases consistent with the fine-tuned regulation of hormonal levels and effects in endocrine axes? Vasoinhibin generation and effects are subject to regulation at the levels defining endocrine axes (Triebel et al., 2015) and the vasoinhibin mode of operation appears neither purely endocrine, paracrine, or autocrine, but instead a combination of them. Advantage of the mixed vasoinhibin mode of operation is taken in clinical studies, in which the pituitary PRL secretion is the target of intervention to stimulate or inhibit retinal or

Table 3
Genetic variant analysis of a cleavage site in PL. Cleavage-site of the 15.7 kDa vasoinhibin-like-peptide generated by plasmin by cleavage of PL between arginine in position 160 and threonine in position 161 with adjacent amino acids. The numbers below the amino acids indicate observed cleavages with the amino acid at the corresponding position in the cleavage site, retrieved from the MEROPS-database. Cleavage occurs between P1 and P1', indicated by the red line. The 8P-score, indicating cleavage efficiency, is 113 in the wt-sequence, but varies with the indicated point mutations, which were retrieved from ENSEMBL on the PL transcript CSH1-201. A lower score than 109 indicates a lower cleavage efficiency, and a higher score a higher cleavage efficiency.

Vi-isoform	Enzyme/Subst.	Amino acid position/P-position/Amino acid/number of observed cleavages (MEROPS)								8P-score	8P-change
15.7 kDa Vasoinhibin-like peptide (from PL)		157	158	159	160	161	162	163	164		
		P4	P3	P2	P1	P1′	P2′	P3′	P4′		
		Gly	Ser	Arg	Arg	Thr	Gly	Gln	Ile		
	Plasmin	10	12	3	65	4	4	8	7	113	
	Gly > Ser	P4	P3	P2	P1	P1′	P2′	P3′	P4′		
	rs1054979309	Ser	Ser	Arg	Arg	Thr	Gly	Gln	Ile		
	Plasmin	8	12	3	65	4	4	8	7	111	−2
	Arg > Pro	P4	P3	P2	P1	P1′	P2′	P3′	P4′		
	rs558064451	Gly	Ser	Pro	Arg	Thr	Gly	Gln	Ile		
	Plasmin	10	12	12	65	4	4	8	7	122	+9
	Arg > His	P4	P3	P2	P1	P1′	P2′	P3′	P4′		
	rs558064451	Gly	Ser	His	Arg	Thr	Gly	Gln	Ile		
	Plasmin	10	12	2	65	4	4	8	7	112	−1
	Arg > Cys	P4	P3	P2	P1	P1′	P2′	P3′	P4′		
	rs577932530	Gly	Ser	Cys	Arg	Thr	Gly	Gln	Ile		
	Plasmin	10	12	2	65	4	4	8	7	112	−1
	Arg > Leu	P4	P3	P2	P1	P1′	P2′	P3′	P4′		
	rs760583471	Gly	Ser	Arg	Leu	Thr	Gly	Gln	Ile		
	Plasmin	10	12	3	0	4	4	8	7	48	−65
	Arg > Gln	P4	P3	P2	P1	P1′	P2′	P3′	P4′		
	rs760583471	Gly	Ser	Arg	Gln	Thr	Gly	Gln	Ile		
	Plasmin	10	12	3	1	4	4	8	7	49	−64
	Arg > Trp	P4	P3	P2	P1	P1′	P2′	P3′	P4′		
	rs764110793	Gly	Ser	Arg	Trp	Thr	Gly	Gln	Ile		
	Plasmin	10	12	3	0	4	4	8	7	48	−65
	Arg > Gly	P4	P3	P2	P1	P1′	P2′	P3′	P4′		
	rs764110793	Gly	Ser	Arg	Gly	Thr	Gly	Gln	Ile		
	Plasmin	10	12	3	0	4	4	8	7	48	−65
	Gly > Arg	P4	P3	P2	P1	P1′	P2′	P3′	P4′		
	rs541688052	Gly	Ser	Arg	Arg	Thr	Arg	Gln	Ile		
	Plasmin	10	12	3	65	4	13	8	7	122	+9
	Ile > Thr	P4	P3	P2	P1	P1′	P2′	P3′	P4′		
	rs771831985	Gly	Ser	Arg	Arg	Thr	Gly	Gln	Thr		
	Plasmin	10	12	3	65	4	4	8	7	113	0
	Ile > Phe	P4	P3	P2	P1	P1′	P2′	P3′	P4′		
	rs1346530698	Gly	Ser	Arg	Arg	Thr	Gly	Gln	Phe		
	Plasmin	10	12	3	65	4	4	8	7	113	0

cardiac vasoinhibin levels in diabetic macular edema and peripartum cardiomyopathy, respectively (Robles-Osorio et al., 2018) (Hilfiker-Kleiner et al., 2017). Also, the differential activity of vasoinhibin in different organs indicates fine-tuned regulation of hormonal and cytokine-like effects (Clapp et al., 2015; Triebel et al., 2015; Yun et al., 2019). Both, specificity and regulation of vasoinhibin generation and effects are compatible with evidence portraying protein hormone fragmentation, and specifically the fragmentation of PRL, as an evolved process that gradually releases factors that alter intracellular or extracellular functions by acting as modulators of metabolic enzymes, transduction factors, protein binding proteins, or hormone receptors (Triebel et al., 2015; Campbell et al., 2021).

Author's note

A poster was presented by JT at the 62. German Congress for Endocrinology, Göttingen, Germany, March 20–22, 2019.

Funding

Supported in part by grant A1-S-9620B from the National Council of Science and Technology of Mexico (CONACYT) to CC.

CRediT author contribution statement

Christin Friedrich: Investigation, Data curation, Formal analysis, Visualization, Writing – review & editing. **Leon Neugebauer:** Investigation, Visualization, Data curation, Writing - review & editing **Magdalena Zamora:** Conceptualization, Investigation, Data curation, Formal analysis, Visualization. **Juan Pablo Robles:** Conceptualization, Investigation, Data curation, Visualization, Formal analysis, Writing - review & editing **Carmen Clapp:** Conceptualization, Data curation, Formal analysis, Writing – review & editing. **Thomas Bertsch:** Conceptualization, Resources, Methodology, Formal analysis, Visualization, Writing – review & editing. **Jakob Triebel:** Conceptualization, Supervision, Project administration, Visualization, Writing – original draft, Data curation, Formal analysis, Methodology, Investigation.

References

Aranda, J., Rivera, J.C., Jeziorski, M.C., Riesgo-Escovar, J., Nava, G., Lopez-Barrera, F., et al., 2005. Prolactins are natural inhibitors of angiogenesis in the retina. Epub 2005/07/27 Investigative ophthalmology & visual science 46 (8), 2947–2953. https://doi.org/10.1167/iovs.05-0173. PubMed PMID: 16043870.

Arnold, E., Rivera, J.C., Thebault, S., Moreno-Paramo, D., Quiroz-Mercado, H., Quintanar Stephano, A., et al., 2010. High levels of serum prolactin protect against diabetic retinopathy by increasing ocular vasoinhibins. Epub 2010/09/09 Diabetes 59 (12), 3192–3197. https://doi.org/10.2337/db10-0873. PubMed PMID: 20823101; PubMed Central PMCID: PMCPMC2992782.

Artimo, P., Jonnalagedda, M., Arnold, K., Baratin, D., Csardi, G., de Castro, E., et al., 2012. ExPASy: SIB bioinformatics resource portal. Web Server issue):W597-603. Epub 2012/06/05 Nucleic Acids Res. 40. https://doi.org/10.1093/nar/gks400. PubMed PMID: 22661580; PubMed Central PMCID: PMCPMC3394269.

Bajou, K., Herkenne, S., Thijssen, V.L., D'Amico, S., Nguyen, N.Q., Bouche, A., et al., 2014. PAI-1 mediates the antiangiogenic and profibrinolytic effects of 16K prolactin.

Epub 2014/06/16 Nat. Med. 20 (7), 741–747. https://doi.org/10.1038/nm.3552. PubMed PMID: 24929950.
Campbell, K.L., Haspel, N., Gath, C., Kurniatash, N., Nouduri Akkiraju, I., Stuffers, N., et al., 2021. Protein hormone fragmentation in intercellular signaling: hormones as nested information systems. Epub 2021/01/07 Biol. Reprod. 104 (4), 887–901. https://doi.org/10.1093/biolre/ioaa234. PubMed PMID: 33403392.
Cao, R., Wu, H.-L., Veitonmäki, N., Linden, P., Farnebo, J., Shi, G.-Y., et al., 1999. Suppression of angiogenesis and tumor growth by the inhibitor K1–5 generated by plasmin-mediated proteolysis. Proc. Natl. Acad. Sci. Unit. States Am. 96 (10), 5728–5733. https://doi.org/10.1073/pnas.96.10.5728.
Clapp, C., Weiner, R.I., 1992. A specific, high affinity, saturable binding site for the 16-kilodalton fragment of prolactin on capillary endothelial cells. PubMed PMID: 1311239 Endocrinology 130 (3), 1380–1386. https://doi.org/10.1210/endo.130.3.1311239. Epub 1992/03/01.
Clapp, C., Thebault, S., Macotela, Y., Moreno-Carranza, B., Triebel, J., Martinez de la Escalera, G., 2015. Regulation of blood vessels by prolactin and vasoinhibins. Epub 2014/12/05 Adv. Exp. Med. Biol. 846, 83–95. https://doi.org/10.1007/978-3-319-12114-7_4. PubMed PMID: 25472535.
Corbacho, A.M., Martinez De La Escalera, G., Clapp, C., 2002. Roles of prolactin and related members of the prolactin/growth hormone/placental lactogen family in angiogenesis. Epub 2002/05/16 J. Endocrinol. 173 (2), 219–238. https://doi.org/10.1677/joe.0.1730219. PubMed PMID: 12010630.
Cruz-Soto, M.E., Cosio, G., Jeziorski, M.C., Vargas-Barroso, V., Aguilar, M.B., Carabez, A., et al., 2009. Cathepsin D is the primary protease for the generation of adenohypophyseal vasoinhibins: cleavage occurs within the prolactin secretory granules. Epub 2009/10/13 Endocrinology 150 (12), 5446–5454. https://doi.org/10.1210/en.2009-0390. PubMed PMID: 19819948.
Duenas, Z., Rivera, J.C., Quiroz-Mercado, H., Aranda, J., Macotela, Y., Montes de Oca, P., et al., 2004. Prolactin in eyes of patients with retinopathy of prematurity: implications for vascular regression. Epub 2004/06/30 Investigative ophthalmology & visual science 45 (7), 2049–2055. https://doi.org/10.1167/iovs.03-1346. PubMed PMID: 15223776.
Ge, G., Fernandez, C.A., Moses, M.A., Greenspan, D.S., 2007. Bone morphogenetic protein 1 processes prolactin to a 17-kDa antiangiogenic factor. Proceedings of the National Academy of Sciences of the United States of America. Epub 2007/06/06, 104 (24), 10010–10015. https://doi.org/10.1073/pnas.0704179104. PubMed PMID: 17548836; PubMed Central PMCID: PMCPMC1891225.
Gonzalez, C., Parra, A., Ramirez-Peredo, J., Garcia, C., Rivera, J.C., Macotela, Y., et al., 2007. Elevated vasoinhibins may contribute to endothelial cell dysfunction and low birth weight in preeclampsia. Epub 2007/08/07 Laboratory investigation; a journal of technical methods and pathology 87 (10), 1009–1017. https://doi.org/10.1038/labinvest.3700662. PubMed PMID: 17676064.
Hilfiker-Kleiner, D., Kaminski, K., Podewski, E., Bonda, T., Schaefer, A., Sliwa, K., et al., 2007. A cathepsin D-cleaved 16 kDa form of prolactin mediates postpartum cardiomyopathy. Epub 2007/02/10 Cell 128 (3), 589–600. https://doi.org/10.1016/j.cell.2006.12.036. PubMed PMID: 17289576.
Hilfiker-Kleiner, D., Haghikia, A., Berliner, D., Vogel-Claussen, J., Schwab, J., Franke, A., et al., 2017. Bromocriptine for the treatment of peripartum cardiomyopathy: a multicentre randomized study. Epub 2017/09/25 Eur. Heart J. 38 (35), 2671–2679. https://doi.org/10.1093/eurheartj/ehx355. PubMed PMID: 28934837; PubMed Central PMCID: PMCPMC5837241.
Ishida, M., Maehara, M., Watanabe, T., Yanagisawa, Y., Takata, Y., Nakajima, R., et al., 2014. Vasoinhibins, N-terminal mouse prolactin fragments, participate in mammary gland involution. Epub 2014/03/07 J. Mol. Endocrinol. 52 (3), 279–287. https://doi.org/10.1530/JME-13-0189. PubMed PMID: 24598201.
Leanos-Miranda, A., Marquez-Acosta, J., Cardenas-Mondragon, G.M., Chinolla-Arellano, Z.L., Rivera-Leanos, R., Bermejo-Huerta, S., et al., 2008. Urinary prolactin as a reliable marker for preeclampsia, its severity, and the occurrence of adverse pregnancy outcomes. Epub 2008/05/08 J. Clin. Endocrinol. Metab. 93 (7), 2492–2499. https://doi.org/10.1210/jc.2008-0305. PubMed PMID: 18460570.
Lenke, L., Martinez de la Escalera, G., Clapp, C., Bertsch, T., Triebel, J., 2019. A dysregulation of the prolactin/vasoinhibin Axis Appears to contribute to preeclampsia. Epub 2020/01/31 Front. Endocrinol. 10, 893. https://doi.org/10.3389/fendo.2019.00893. PubMed PMID: 31998232; PubMed Central PMCID: PMCPMC6962103.
Li, C.H., Graf, L., 1974. Human pituitary growth hormone: isolation and properties of two biologically active fragments from plasmin digests. Epub 1974/04/01 Proceedings of the National Academy of Sciences of the United States of America 71 (4), 1197–1201. https://doi.org/10.1073/pnas.71.4.1197. PubMed PMID: 4275394; PubMed Central PMCID: PMCPMC388191.
Macotela, Y., Aguilar, M.B., Guzman-Morales, J., Rivera, J.C., Zermeno, C., Lopez-Barrera, F., et al., 2006. Matrix metalloproteases from chondrocytes generate an antiangiogenic 16 kDa prolactin. Epub 2006/04/13 J. Cell Sci. 119 (Pt 9), 1790–1800. https://doi.org/10.1242/jcs.02887. PubMed PMID: 16608881.
Mejia, S., Torner, L.M., Jeziorski, M.C., Gonzalez, C., Morales, M.A., de la Escalera, G.M., et al., 2003. Prolactin and 16K prolactin stimulate release of vasopressin by a direct effect on hypothalamo-neurohypophyseal system. Epub 2003/04/02 Endocrine 20 (1–2), 155–162. https://doi.org/10.1385/ENDO:20:1-2:155. PubMed PMID: 12668881.
Morohoshi, K., Mochinaga, R., Watanabe, T., Nakajima, R., Harigaya, T., 2018. 16 kDa vasoinhibin binds to integrin alpha5 beta1 on endothelial cells to induce apoptosis. Epub 2018/04/07 Endocrine connections 7 (5), 630–636. https://doi.org/10.1530/EC-18-0116. PubMed PMID: 29622663; PubMed Central PMCID: PMCPMC5919937.
Nakajima, R., Ishida, M., Kamiya, C.A., Yoshimatsu, J., Suzuki, M., Hirota, A., et al., 2015. Elevated vasoinhibin derived from prolactin and cathepsin D activities in sera of patients with preeclampsia. Epub 2015/09/18 Hypertens. Res. 38 (12), 899–901. https://doi.org/10.1038/hr.2015.99. PubMed PMID: 26376948.
Perimenis, P., Bouckenooghe, T., Delplanque, J., Moitrot, E., Eury, E., Lobbens, S., et al., 2014. Placental antiangiogenic prolactin fragments are increased in human and rat maternal diabetes. Epub 2014/07/02 Biochim. Biophys. Acta 1842 (9), 1783–1793. https://doi.org/10.1016/j.bbadis.2014.06.026. PubMed PMID: 24984282.
Piwnica, D., Touraine, P., Struman, I., Tabruyn, S., Bolbach, G., Clapp, C., et al., 2004. Cathepsin D processes human prolactin into multiple 16K-like N-terminal fragments: study of their antiangiogenic properties and physiological relevance. Epub 2004/06/12 Mol. Endocrinol. 18 (10), 2522–2542. https://doi.org/10.1210/me.2004-0200. PubMed PMID: 15192082.
Rawlings, N.D., Barrett, A.J., Thomas, P.D., Huang, X., Bateman, A., Finn, R.D., 2018. The MEROPS database of proteolytic enzymes, their substrates and inhibitors in 2017 and a comparison with peptidases in the PANTHER database. Epub 2017/11/18 Nucleic Acids Res. 46 (D1), D624–D632. https://doi.org/10.1093/nar/gkx1134. PubMed PMID: 29145643; PubMed Central PMCID: PMCPMC5753285.
Robles, J.P., Zamora, M., Velasco-Bolom, J.L., Tovar, M., Garduno-Juarez, R., Bertsch, T., et al., 2018. Vasoinhibin comprises a three-helix bundle and its antiangiogenic domain is located within the first 79 residues. Epub 2018/11/22 Sci. Rep. 8 (1), 17111. https://doi.org/10.1038/s41598-018-35383-7. PubMed PMID: 30459448; PubMed Central PMCID: PMCPMC6244167.
Robles-Osorio, M.L., Garcia-Franco, R., Nunez-Amaro, C.D., Mira-Lorenzo, X., Ramirez-Neria, P., Hernandez, W., et al., 2018. Basis and design of a randomized clinical trial to evaluate the effect of levosulpiride on retinal alterations in patients with diabetic retinopathy and diabetic macular edema. Epub 2018/06/14 Front. Endocrinol. 9, 242. https://doi.org/10.3389/fendo.2018.00242. PubMed PMID: 29896154; PubMed Central PMCID: PMCPMC5986911.
Sinha, Y.N., Ott, K., Vanderlaan, W.P., 1987. Detection of multiple PRL- and GH-like proteins in human pituitary by Western blot analysis. Epub 1987/07/01 Am. J. Med. Sci. 294 (1), 15–25. https://doi.org/10.1097/00000441-198707000-00003. PubMed PMID: 3300328.
Song, J., Tan, H., Perry, A.J., Akutsu, T., Webb, G.I., Whisstock, J.C., et al., 2012. PROSPER: an integrated feature-based tool for predicting protease substrate cleavage sites. Epub 2012/12/05 PloS One 7 (11), e50300. https://doi.org/10.1371/journal.pone.0050300. PubMed PMID: 23209700; PubMed Central PMCID: PMCPMC3510211.
Struman, I., Bentzien, F., Lee, H., Mainfroid, V., D'Angelo, G., Goffin, V., et al., 1999. Opposing actions of intact and N-terminal fragments of the human prolactin/growth hormone family members on angiogenesis: an efficient mechanism for the regulation of angiogenesis. Epub 1999/02/17 Proceedings of the National Academy of Sciences of the United States of America 96 (4), 1246–1251. https://doi.org/10.1073/pnas.96.4.1246. PubMed PMID: 9990009; PubMed Central PMCID: PMCPMC15448.
Triebel, J., Huefner, M., Ramadori, G., 2009. Investigation of prolactin-related vasoinhibin in sera from patients with diabetic retinopathy. Epub 2009/05/30 Eur. J. Endocrinol./European Federation of Endocrine Societies 161 (2), 345–353. https://doi.org/10.1530/EJE-09-0130. PubMed PMID: 19477896.
Triebel, J., Macotela, Y., de la Escalera, G.M., Clapp, C., 2011. Prolactin and vasoinhibins: endogenous players in diabetic retinopathy. Epub 2011/09/14 IUBMB Life 63 (10), 806–810. https://doi.org/10.1002/iub.518. PubMed PMID: 21913303.
Triebel, J., Bertsch, T., Bollheimer, C., Rios-Barrera, D., Pearce, C.F., Hufner, M., et al., 2015. Principles of the prolactin/vasoinhibin axis. Epub 2015/08/28 Am. J. Physiol. Regul. Integr. Comp. Physiol. 309 (10), R1193–R1203. https://doi.org/10.1152/ajpregu.00256, 2015. PubMed PMID: 26310939; PubMed Central PMCID: PMCPMC4666935.
Triebel, J., Friedrich, C.J., Leuchs, A., Martinez de la Escalera, G., Clapp, C., Bertsch, T., 2017a. Human prolactin point mutations and their projected effect on vasoinhibin generation and vasoinhibin-related diseases. Epub 2017/11/23 Front. Endocrinol. 8 (294), 294. https://doi.org/10.3389/fendo.2017.00294. PubMed PMID: 29163363; PubMed Central PMCID: PMCPMC5681482.
Triebel, J., Martinez de la Escalera, G., Clapp, C., Bertsch, T., 2017b. Vasoinhibins may contribute to postpartum depression. Epub 2017/09/29 Front Psychiatry 8, 167. https://doi.org/10.3389/fpsyt.2017.00167. PubMed PMID: 28955253; PubMed Central PMCID: PMCPMC5600915.
Triebel, J., Silawal, S., Willauschus, M., Schulze-Tanzil, G., Bertsch, T., 2019. Analysing point mutations in protein cleavage sites by using enzyme specificity matrices. Epub 2019/05/28 Front. Endocrinol. 10, 267. https://doi.org/10.3389/fendo.2019.00267. PubMed PMID: 31130917; PubMed Central PMCID: PMCPMC6509992.
Yun, B.Y., Cho, C., Cho, B.N., 2019. Differential activity of 16K rat prolactin in different organic systems. Epub 2019/04/06 Anim. Cell Syst. 23 (2), 135–142. https://doi.org/10.1080/19768354.2018.1554543. PubMed PMID: 30949401; PubMed Central PMCID: PMCPMC6440500.
Zamorano, M., Ledesma-Colunga, M.G., Adan, N., Vera-Massieu, C., Lemini, M., Mendez, I., et al., 2014. Prolactin-derived vasoinhibins increase anxiety- and depression-related behaviors. Epub 2014/04/29 Psychoneuroendocrinology 44, 123–132. https://doi.org/10.1016/j.psyneuen.2014.03.006. PubMed PMID: 24767626.
Epub 2017/11/21 Zerbino, D.R., Achuthan, P., Akanni, W., Amode, M.R., Barrell, D., Bhai, J., et al., 2018. Ensembl, 2018 Nucleic Acids Res. 46 (D1), D754–D761. https://doi.org/10.1093/nar/gkx1098. PubMed PMID: 29155950; PubMed Central PMCID: PMCPMC5753206.